PERGAMON

Journal of Structural Geology 23 (2001) 25–32

JOURNAL OF STRUCTURAL GEOLOGY

www.elsevier.nl/locate/jstrugeo

The distribution of deformation in parallel fault-related folds with migrating axial surfaces: comparison between fault-propagation and fault-bend folding

Francesco Salvini*, Fabrizio Storti

Dipartimento di Scienze Geologiche, Università degli Studi "Roma Tre", Largo S. L. Murialdo 1, 00146 Roma, Italy

Received 19 October 1999; accepted 5 June 2000

Abstract

In fault-related folds that form by axial surface migration, rocks undergo deformation as they pass through axial surfaces. The distribution and intensity of deformation in these structures has been impacted by the history of axial surface migration. Upon fold initiation, unique dip panels develop, each with a characteristic deformation intensity, depending on their history. During fold growth, rocks that pass through axial surfaces are transported between dip panels and accumulate additional deformation. By tracking the pattern of axial surface migration in model folds, we predict the distribution of relative deformation intensity in simple-step, parallel fault-bend and fault-propagation anticlines. In both cases the deformation is partitioned into unique domains we call deformation panels. For a given rheology of the folded multilayer, deformation intensity will be homogeneously distributed in each deformation panel. Fold limbs are always deformed. The flat crests of fault-propagation anticlines are always undeformed. Two asymmetric deformation panels develop in fault-propagation folds above ramp angles exceeding 29°. For lower ramp angles, an additional, more intensely-deformed panel develops at the transition between the crest and the forelimb. Deformation in the flat crests of fault-bend anticlines occurs when fault displacement exceeds the length of the footwall ramp, but is never found immediately hinterland of the crest to forelimb transition. In environments dominated by brittle deformation, our models may serve as a first-order approximation of the distribution of fractures in fault-related folds.

1. Introduction

The distribution of mesoscopic deformation features in fault-related folds has important consequences for hydrocarbon migration, trapping and production. Pressure solution cleavage, deformation bands and joints may enhance or retard fluid flow and can impart significant permeability anisotropy. Structural, environmental and stratigraphic factors control the spatial distribution and intensity of these deformation features (e.g. Fischer and Jackson, 1999). In fault-related folds developing in a rock sequence with a given mechanical stratigraphy (e.g. Corbett et al., 1987; Woodward and Rutherford, 1989; Gutierrez-Alonso and Gross, 1999) and in given environmental conditions (e.g. Stewart and Alvarez, 1991; Jamison, 1992; Lemiszki et al., 1994), the distribution of deformation is mainly controlled by fault-fold kinematics (e.g. Sanderson, 1982; Fischer et al., 1992; Storti and Salvini, 1996).

Fault-related folding mechanisms can generally be divided into two categories (Stewart and Alvarez, 1991): those involving limb rotation about fixed axial surfaces (e.g. De Sitter, 1956) (fixed-hinge folding) and those involving the lateral migration of active axial surfaces (e.g. Suppe, 1983) (active-hinge folding). Fixed and active terms are relative to an internal coordinate frame. Diagnostic distributions of deformation are expected for the two end-member folding mechanisms and have been used to infer the fold kinematics (e.g. Beutner and Diegel, 1985; Stewart and Alvarez, 1991; Fischer et al., 1992; Fisher and Anastasio, 1994; Hedlund et al., 1994; Anastasio et al., 1997; Erslev and Mayborn, 1997; Thorbjornsen and Dunne, 1997).

In this paper we predict the time-space distribution of deformation intensity, i.e. the degree to which rocks are deformed (Fischer and Jackson, 1999), in simple-step parallel fault-bend and fault-propagation anticlines. We assume that deformation is entirely controlled by model fold kinematics as described by Suppe (1983) and Suppe and Medwedeff (1990). We show that, in contrast with classical models based on fixed-hinge folding, fold limbs in fault-bend and fault-propagation anticlines are preferred sites

* Corresponding author.
E-mail address: salvini@uniroma3.it (F. Salvini).

0191-8141/01/$ - see front matter
PII: S0191-8141(00)00081-X

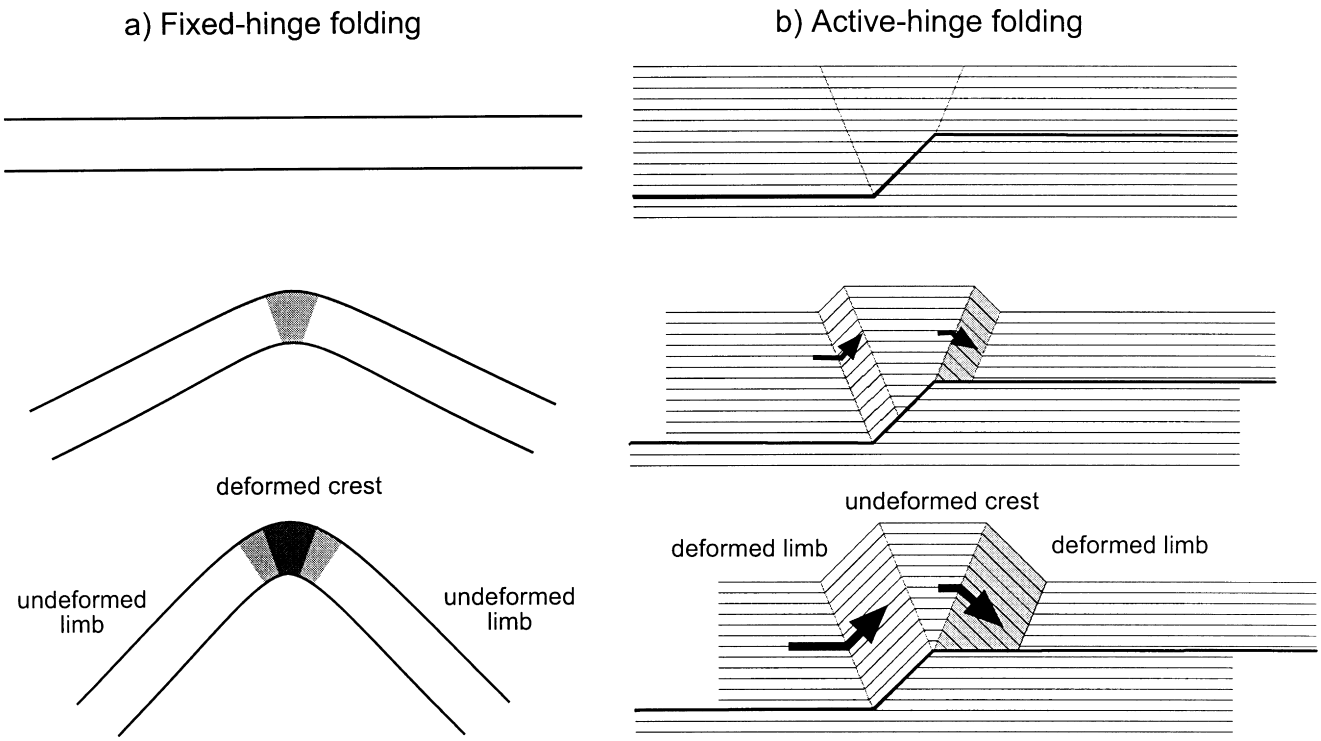

Fig. 1. Contrasting spatial distribution of deformation associated to fixed-hinge folding (a) and active-hinge folding (b) respectively.

for deformation, rather than the corresponding anticlinal crests, which are characterised by more complex evolutionary paths.

2. Deformation in active versus fixed-hinge folding

The differences in the time-spatial evolution of deformation between active- and fixed-hinge folding are highlighted in Fig. 1. In fixed-hinge folds (Fig. 1a) deformation concentrates in the axial surface area and, as the fold develops, the dimensions of the deformed zone do not significantly increase. Deformation intensity concentrates in the hinge zone and decreases towards the limbs. A correspondence between layer curvature and deformation intensity is expected, with the maximum deformation intensity at the fold hinges (e.g. Dieterich and Carter, 1969; Ramsay, 1974).

Deformation in migrating-hinge folds follows an almost opposite path (Fig. 1b). Since the deformation develops in the hangingwall rocks as they pass through the active axial surfaces (e.g. Evans and Dunne, 1991; Stewart and Alvarez, 1991; Fischer et al., 1992; Hedlund et al., 1994; Erickson and Jamison, 1995; Apotria et al., 1996; Storti and Salvini, 1996), deformation is concentrated in the limbs of the structures, leaving the crest of the fold unaffected. Continued folding and fault slip produces an increase in the dimensions of these deformed rock panels. For a given rheology of the rock multilayer, deformation intensity may be assumed to depend on the angle, number and sense of rotation (e.g. Storti and Salvini, 1996). Rock panels that underwent homogeneously distributed deformation by parallel folding are hereafter referred to as deformation panels. Deformation intensity is expected to be nearly constant within a deformation panel. The progressive geometric changes of folded rock panels during continued fault slip cause correspondent variations in the distribution of deformation panels.

3. Deformation patterns in parallel fault-propagation anticlines

In fault-propagation folding (Suppe and Medwedeff, 1984) layers are successively folded and then faulted as fault displacement increases and the length of the blind thrust ramp increases (Fig. 2). In the simplest case (simple-step, Suppe and Medwedeff, 1990) a single anticlinal axial surface develops in the faulted layers (C in Fig. 2), and then bifurcates upward to form axial surfaces A and B' in the folded layers. The bifurcation point is located at the same stratigraphic elevation as the fault tip. Axial surfaces A, A', B, and B' are active, and C is inactive (Mosar and Suppe, 1992). With increasing shortening, axial surface C lengthens, and axial surface B remains constant, whereas axial surfaces A, A' and B' shorten. This causes fold limbs to widen, while the crest width progressively decreases during propagation of the thrust tip.

The kinematics of parallel fault-propagation folding depends on the step-up angle of the blind thrust (Suppe and Medwedeff, 1990). At high fault angles (open and

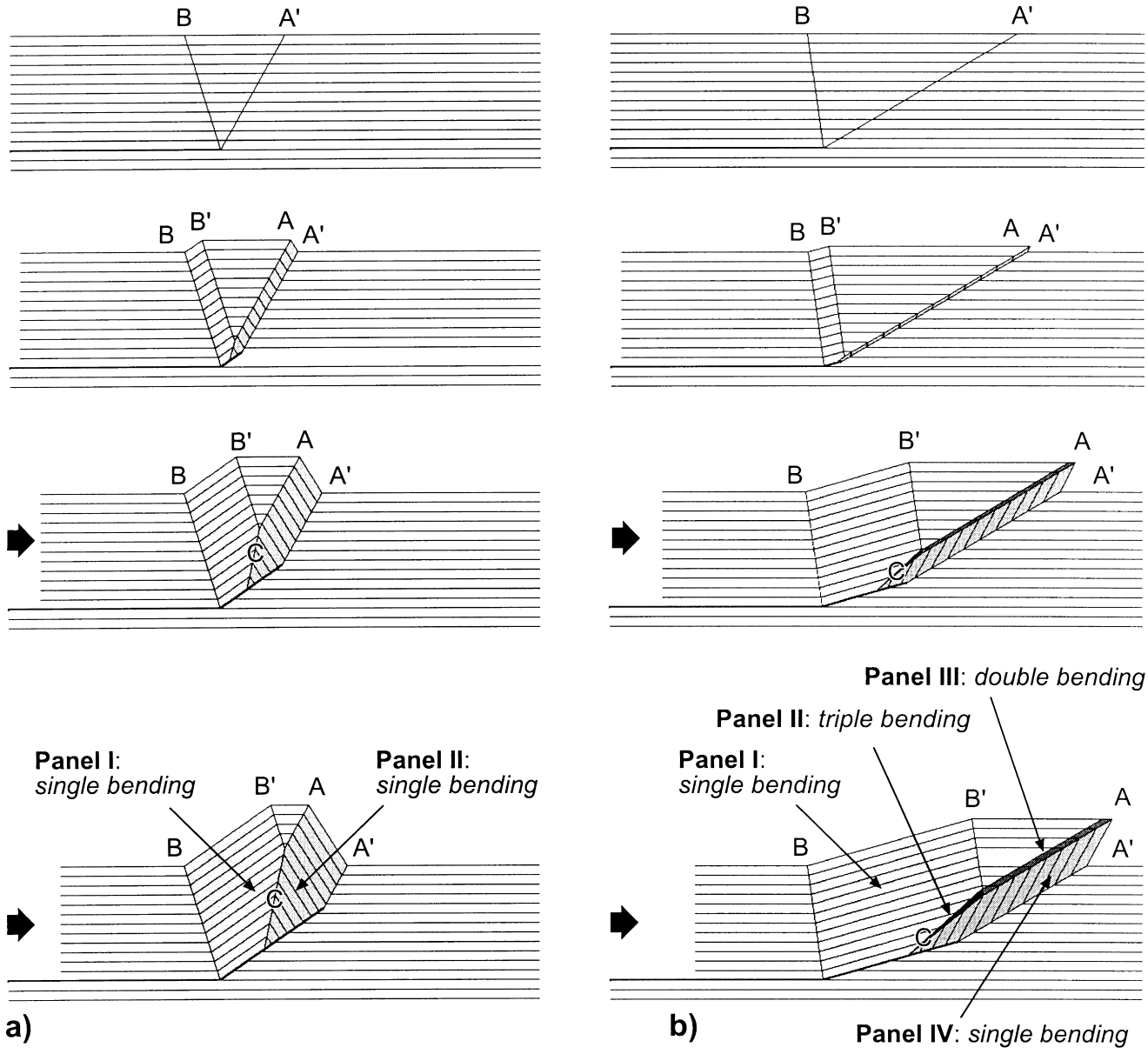

Fig. 2. Sequential development of deformation panels during constant thickness right-way up (a) and overturned (b), fault-propagation folding. Development of deformation panels II and III in overturned fault-propagation folds provides a narrow, weakness zone suitable to trigger anticlinal breaktrough. Note how the crests of the anticlines has no predicted fold-related deformation.

upright folds) material migrates from the crest into the forelimb, whereas at low fault angles (tight and overturned folds) material is transported from the forelimb into the crest with increasing fault slip. When the ramp angle is greater than approximately 29°, widening of the forelimb occurs by including material from both the foreland and the crest (Fig. 2a), the relative amount being a function of the ramp angle itself. The expected deformation intensity is the same for material transported through axial surfaces A and A' because the bending angle is the same. With continued fault slip, the forelimb and backlimb develop unique, widening deformation panels while the flat-lying crest remains undeformed and progressively narrows. Ramp angles lower than approximately 41° require that the forelimb is steeper and, consequently, more intensely deformed than the backlimb. When the ramp angle exceeds 41° the asymmetry of the thrust-tip anticline becomes opposite to the tectonic transport direction and fracture intensity is expected to be higher in the backlimb.

For ramp angles lower than about 29°, lengthening of the forelimb is achieved by the upward translation of foreland material through axial surface A'. Deformed material in the forelimb then migrates into the crest by passing through active axial surface A, and apparently unfolds because it undergoes an additional bending of the same amount, but in the opposite direction. An intensely deformed sector

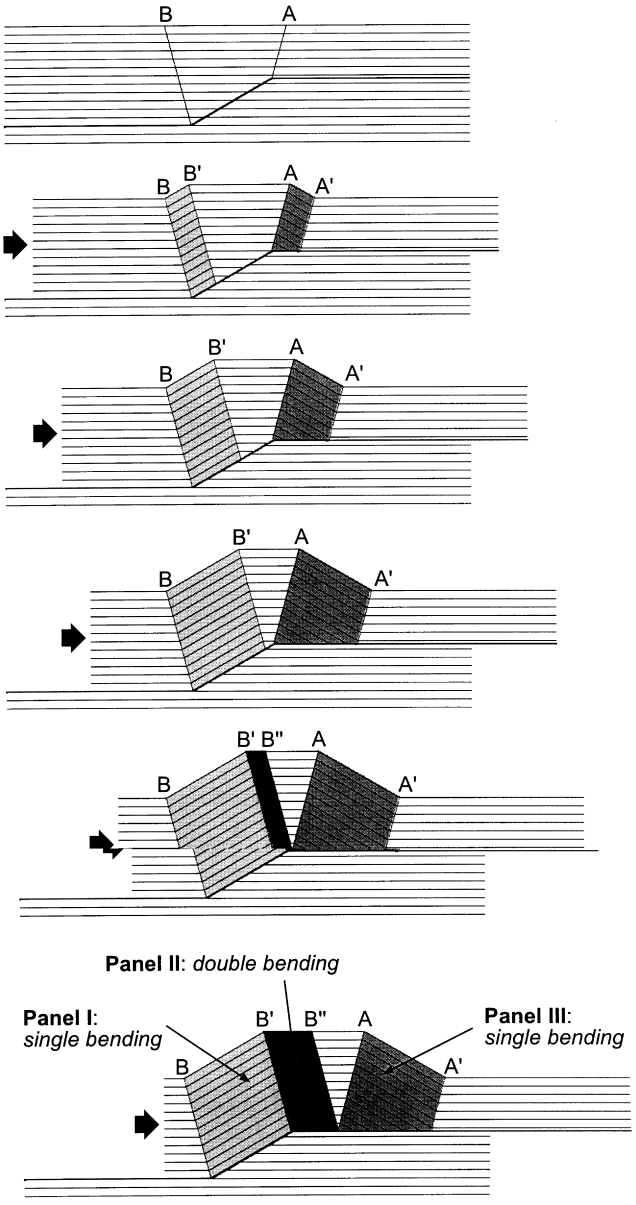

Fig. 3. Sequential development of deformation panels during simple step fault-bend folding. Notice how fold limbs are always deformed while the whole anticlinal crest remains undeformed until axial surface B'' develops, after that deformation panel II develops.

originates at the front of the flat-lying crest (panel III in Fig. 2b) and its width depends on the ramp angle. The upward migration of the bifurcation point at the tip of axial surface C causes a third slight bending of this highly deformed sector by passing through axial surface B'. This causes a downward narrowing, highly deformed zone adjacent to the axial surface C (panel II in Fig. 2b). Four deformation panels develop during growth of a low-angle fault-propagation anticline (Fig. 2b). Deformation intensity due to folding is expected to be higher in the forelimb than the backlimb, due to the different amount of rotation of the hangingwall rocks as they migrate through the axial surfaces.

4. Comparison with parallel fault-bend anticlines

The kinematics of fault-bend folding has been fully described (e.g. Suppe, 1983, Wilkerson et al., 1991; Hedlund et al., 1994; Hardy, 1995; Medwedeff and Suppe, 1997) and deformation patterns have been numerically modelled (e.g. Erickson and Jamison, 1995; Strayer and Hudleston, 1997). Material in the rear of a fault-bend anticline (Fig. 3) passes through the axial surface B, which is pinned at the lower ramp inflection point, and is deformed while transported upward along the footwall ramp. Simultaneously in the crest of the fold, material passes through the axial surface A, which is pinned at the upper ramp inflection point, and deforms while entering the forelimb. The additional boundaries between deformed and undeformed material are given by the inactive (Suppe et al., 1992) axial surfaces, i.e. those fixed in the hangingwall material (B' and A' in Fig. 3). Two deformation panels develop in the backlimb and forelimb of a fault-bend anticline when the amount of fault slip is small. The flat-lying crest is virtually undeformed and progressively decreases in width until axial surface B' reaches the upper ramp inflection point and pins there, becoming active. Material unfolds during translation along the upper flat (Suppe, 1983). This folding to an apparent, unfolded state occurs by refolding the previously deformed backlimb material when it migrates into the crest across axial surface B'. Consequently, a new, more intensely deformed panel develops in the crest, whose forelandward boundary (B'') is parallel to B' and joins A at the base. Boundaries B'' and A define a virtually undeformed inverted triangle, whose constant width depends on the initial thickness of the deformed multilayer and the cut-off angle. With increasing fault slip three deformation panels occur (Fig. 3): the width of panels BB' and AA' remains constant, while panel B'B'' progressively widens. When fault displacement is much greater than the length of the ramp, the wider and more intensely deformed panel in fault-bend anticlines locates in the anticlinal crest.

The deformation pattern in small-displacement fault-bend anticlines resembles that of fault-propagation anticlines having a ramp angle greater than about 29° and consists of two deformation panels (compare Fig. 2a and Fig. 3). The third, more intensely deformed crestal panel that characterises the late-stage evolution of fault-bend folds does not develop in fault-propagation folds. Fault-propagation anticlines developing ahead of shallowly-dipping thrust ramps have a diagnostic deformation pattern.

5. Discussion

5.1. Fault-fold kinematics

Our model results relate to the kinematics of folding. Deformation patterns are specific to the folding mechanism. This is particularly true for fault-propagation folding, for

which different geometric and kinematic models have been proposed (e.g. Jamison, 1987; Chester and Chester, 1990; Mitra, 1990; Suppe and Medwedeff, 1990; Erslev, 1991; Wickham, 1995; Storti and Salvini, 1996).

The intensely-deformed panel developed in fault-propagation folds (Suppe and Medwedeff, 1990) above ramp angles lower than 30° may provide one mechanical explanation for the common occurrence of anticlinal breakthrough and the preservation of footwall synclines in thrust-fold belts. Such a heavily-deformed, narrow band at the crest-forelimb transition (Fig. 2b) may provide a pathway weaker than the region at the tip of the master blind ramp, and this may trigger the emanation of a splay thrust in the anticlinal core and its rapid upward propagation. This produces further deformation in the hangingwall rocks, where new deformation panels originate (Fig. 4a).

Because we used a number of simplifying assumptions, our models develop rather elementary deformation patterns. We purposely chose simple geometries and kinematics to emphasize the processes by which deformation panels develop and evolve. More complex kinematic models (e.g. multi-mode fault-propagation folding, Erslev and Mayborn, 1997; multibend fault-bend folding, Medwedeff and Suppe, 1997) will produce more complex distributions and interference patterns of deformation panels. For example, the kinematic models we used assume that axial surfaces migrate self-similarly and do not rotate during fold amplification (mode I of Weiss, 1980). Different evolutionary models of axial surface migration or their combination (e.g. Stewart and Alvarez, 1991 and references therein) will produce different and more complex deformation patterns. Fold kinematics may also vary through time; we maintained the same fold kinematics through time. Fold kinematics may change with increasing fault slip (e.g. Dixon and Liu, 1992; McNaught and Mitra, 1993; Storti et al., 1997), resulting in the superimposition of different deformation panels.

In addition to more complex fold kinematics or fault geometries, boundary stress conditions influence the competition between folding and faulting. Different kinematic mechanisms of fault-related folding are predicted at different depths (e.g. Jamison, 1992), and will consequently be characterised by different deformation panels. The depth of burial among many other intrinsic and extrinsic parameters also influences deformation styles within the folded rock panels (e.g. Lemiszki et al., 1994). Tensile fracturing is favoured at shallow depths and solution and shear cleavages are favoured at increasing confining pressures.

5.2. Mechanical stratigraphy

Our models assume deformation of isotropic material. This is an oversimplification of the natural behaviour of rocks, that are commonly layered. Rock multilayers are characterised by a strong mechanical anisotropy and this influences the deformation style and the evolution of the deformation mechanisms in space and time (e.g. Woodward and Rutherford, 1989; Erickson and Jamison, 1995; Fischer and Jackson, 1999; Gutierrez-Alonso and Gross, 1999). However, mechanical stratigraphy is likely to play a subordinate role in the spatial distribution of deformation panels, since in active-hinge folding the spatial distribution mainly depends on the three-dimensional geometric array of axial surfaces and on the amount of fault slip. This means that identical active-hinge folds developed by the same kinematics in multilayers with different mechanical stratigraphies, are expected to show similar distributions of deformation panels, but different deformation styles, mechanisms, and intensities within the corresponding deformation panels.

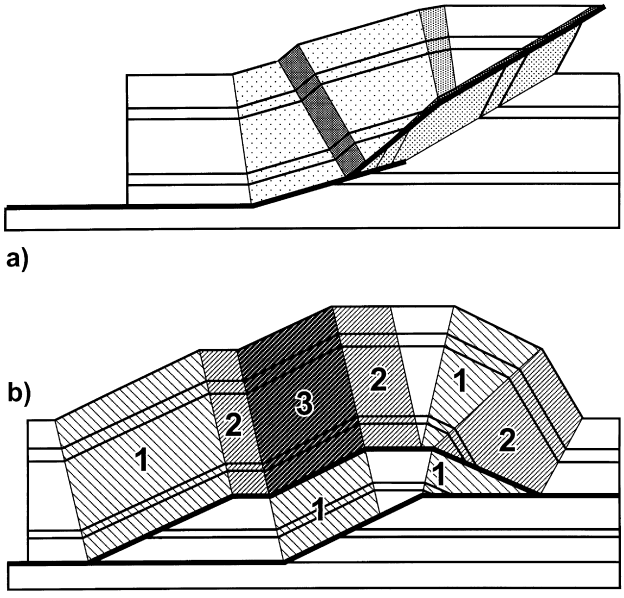

Fig. 4. (a) Anticlinal breakthrough in a fault-propagation anticline, along the highly deformed elongated panel in the fold core; the intensity of shading is proportional to the intensity of deformation. (b) Example of a more complex distribution of deformation panels in a contractional structure developed by fault-bend folding; numbers indicate the number of bendings the patterned panels underwent. White areas are unfolded.

5.3. Insights for folding-related fracturing

The deformation style in deformation panels developed at shallow depths includes mostly extensional and shear fractures, pressure solution and small-scale faults (e.g. Wiltschko et al., 1985; Wojtal, 1986; Wojtal and Mitra, 1986; Stewart and Alvarez, 1991; Holl and Anastasio, 1992) hereafter all referred to as fractures. Fractures in fault-related folds are generally arranged in two main sets: longitudinal fractures (Mitra, 1987), almost aligned with the fold axis, and transverse fractures (Mitra, 1987), trending almost perpendicular to the fold axis and including conjugate arrays (e.g. Price, 1966; Stearns, 1968; Cooper, 1992). Longitudinal fractures are commonly interpreted as being

produced by bending during folding (e.g. Dahlstrom, 1990; Srivastava and Engelder, 1990; Cooper, 1992; Lemiszki et al., 1994; Apotria et al., 1996; Cacas et al., 1996; Storti and Salvini, 1996; Gibbs et al., 1997; Jamison, 1997; Salvini and Storti, 1997). Longitudinal fractures have an important role in hydrocarbon exploration and development because they can impart a significant directional bias to connectivity (e.g. Narr and Currie, 1982; Jamison, 1997). Deformation panels in our models may provide templates for the location in cross section of the longitudinally fractured zones in surface anticlines. In contrast with classical models based on fixed-hinge folding, fold limbs in fault-bend and fault-propagation anticlines are preferred sites for fracturing, rather than the corresponding anticlinal crests, which remain almost uneffected by longitudinal fracturing in fault-propagation folding and show a two-stage evolution in fault-bend folding (see Figs. 2 and 3). The occurrence of the highest production rates in the limbs of many fault-related reservoir anticlines is in agreement with our results (e.g. Murray, 1968; Apotria et al., 1996). High production rates in part of the crest of fault-bend anticlines may occur and relate to refolding of previously fractured material from the back-limb (panel II in Fig. 3).

5.4. Insights for further work

The correspondence among fault-fold kinematics, fault slip and the distribution of deformation can be used to predict the architecture of deformation panels in complex structures developed by active-hinge folding (Fig. 4b). When the depth of burial, the mechanical stratigraphy and the fabric related to layer-parallel shortening pre-dating folding are taken into account, the complexity of the spatial distribution of deformation panels in the same structure increases.

Deformation intensity in multibent rock panels that developed at shallow depths (i.e. mainly fracturing) is expected to show a saturation limit, mainly controlled by the stress conditions and the rock rheology (e.g. Becker and Gross, 1996). Additional deformation will probably occur by the re-activation of the pre-existing structural fabric. The inclusion of such a non-linear relationship between the number of folding episodes and fracture intensity in heavily deformed, brittle rock panels will further improve the predictive capability of forward modelling tools, particularly for hydrocarbon exploration and development.

The use of self-constraining kinematic models will significantly improve the simulation of natural fault-related folding processes by eliminating the externally-imposed, geometric constraints that characterise fault-bend, fault-propagation, and décollement folding. Such forward modelling tools, including a multilayered stratigraphy, are expected to provide a deformation pattern closer to the natural ones, and are the subject of our ongoing research.

6. Conclusions

1. In active-hinge fault-related anticlines, correspondence exists between fault geometry and slip, fold kinematics and geometry, and the number and geometry of deformed rock panels produced by migration of material through active axial surfaces (deformation panels).
2. Forward modelling of deformation panels developed in fault-propagation folding shows that fold limbs are always deformed, while the flat crest is mostly undeformed. Two asymmetric deformation panels develop in fault-propagation folds above ramp angles exceeding 29°. For lower ramp angles, an additional, more intensely-deformed panel develops at the transition between the crest and the forelimb. In fault-bend folding, fold limbs are always deformed while deformation in the crest occurs when fault displacement exceeds the length of the footwall ramp, but is never found immediately hinterland of the crest to forelimb transition.
3. Our results provide first-order templates for predicting the spatial distribution of longitudinal fracturing in shallow-level fault-related folds. These fractures represent the main cause of permeability in many carbonate reservoirs.

Acknowledgements

Revisions of early versions of the paper by J. P. Evans, M. P. Fischer, D. Fisher, and two anonymous referees allowed us to considerably improve it. In particular, detailed review and constructive criticism from M. P. Fischer greatly contributed to a significant improvement of the paper. This work has been funded by the Italian Ministry of the University and Scientific Research (grants to F. Salvini).

References

Anastasio, D.J., Fisher, D.M., Messina, T.A., Holl, J.E., 1997. Kinematics of decollement folding in the Lost-River Range, Idaho. Journal of Structural Geology 19, 355–368.

Apotria, T.G., Wilkerson, M.S., Knewtson, S.L., 1996. 3D geometry and controls on fracturing in a natural fault-bend fold: Rosario Field, Maracaibo Basin, Venezuela. American Association of Petroleum Geologists Bulletin 80, 1268.

Becker, A., Gross, M.R., 1996. Mechanics for joint saturation in mechanically layered rocks: an example from southern Israel. Tectonophysics 257, 223–237.

Beutner, E.C., Diegel, F.A., 1985. Determination of fold kinematics from syntectonic fibers in pressure shadows, Martinsburg slate, New Jersey. American Journal of Science 285, 16–50.

Cacas, M.C., Letouzey, J., Badsi, M., 1996. Application of an integrated technique for analysing naturally fractured reservoirs. American Association of Petroleum Geologists Bulletin 80, 1278.

Chester, J.S., Chester, F.M., 1990. Fault-propagation folds above thrusts with constant dip. Journal of Structural Geology 12, 903–910.

Cooper, M., 1992. The analysis of fracture systems in subsurface thrust

structures from the foothills of the Canadian Rockies. In: McClay, K.R. (Ed.), Thrust Tectonics. Chapman and Hall, London, pp. 391–405.
Corbett, K., Friedmean, M., Spang, J., 1987. Fracture development and mechanical stratigraphy of Austin Chalk, Texas. American Association of Petroleum Geologists Bulletin 71, 17–28.
Dahlstrom, C.D.A., 1990. Geometric constraints derived from the law of conservation of volume and applied to evolutionary models for detachment folding. American Association of Petroleum Geologists Bulletin 74, 336–344.
De Sitter, L.V., 1956. Structural Geology. McGraw-Hill, New York.
Dieterich, J.H., Carter, N.L., 1969. Stress history of folding. American Journal of Science 267, 129–154.
Dixon, J.M., Liu, S., 1992. Centrifuge modelling of the propagation of thrust faults. In: McClay, K.R. (Ed.), Thrust Tectonics. Chapman and Hall, London, pp. 53–69.
Erickson, S.G., Jamison, W.R., 1995. Viscous-plastic finite-element models of fault-bend folds. Journal of Structural Geology 17, 561–573.
Erslev, E.A., 1991. Trishear fault-propagation folding. Geology 19, 617–620.
Erslev, E.A., Mayborn, K.R., 1997. Multiple geometries and modes of fault-propagation foldin in the Canadian thrust belt. Journal of Structural Geology 19, 321–335.
Evans, M.A., Dunne, W.M., 1991. Strain factorization and partitioning in the North Mountain thrust sheet, central Appalachians, U.S.A. Journal of Structural Geology 13, 21–35.
Fisher, D.M., Anastasio, D.J., 1994. Kinematic analysis of a large scale leading edge fold, Lost River Range, Idaho. Journal of Structural Geology 16, 337–354.
Fischer, M.P., Jackson, P.B., 1999. Stratigraphic controls on deformation patterns in fault-related folds: a detachment fold example from the Sierra Madre Oriental, northeast Mexico. Journal of Structural Geology 21, 613–633.
Fischer, M.P., Woodward, N.B., Mitchell, M.M., 1992. The kinematics of break-thrust folds. Journal of Structural Geology 14, 451–460.
Gibbs, A.D., Jaffri, F., Murray, T., 1997. New techniques for fracture distribution and prediction from kinematic modelling of 3D strain fields. American Association of Petroleum Geologists and Society of Economic Paleontologists and Mineralogists Annual Meeting, Abstracts 6, 40.
Gutierrez-Alonso, G., Gross, M.R., 1999. Structures and mechanisms associated with development of a fold in the Cantabrian Zone thrust belt, NW Spain. Journal of Structural Geology 21, 653–670.
Hardy, S., 1995. A method for quantifying the kinematics of fault-bend folding. Journal of Structural Geology 17, 1785–1788.
Hedlund, C.A., Anastasio, D.J., Fisher, D.M., 1994. Kinematics of fault-related folding in a duplex, Lost River Range, Idaho, U.S.A. Journal of Structural Geology 16, 571–584.
Holl, J.E., Anastasio, D.J., 1992. Deformation of a foreland carbonate thrust system, Sawtooth Range, Montana. Geological Society of America Bulletin 104, 944–953.
Jamison, W.R., 1987. Geometric analysis of fold development in overthrust terranes. Journal of Structural Geology 9, 207–219.
Jamison, W.R., 1992. Stress controls on fold thrust style. In: McClay, K.R. (Ed.), Thrust Tectonics. Chapman and Hall, London, pp. 155–164.
Jamison, W.R., 1997. Quantitative evaluation of fractures on Monkshood Anticline, a detachment fold in the foothills of western Canada. American Association of Petroleum Geologists Bulletin 81, 1110–1132.
Lemiszki, P.J., Landes, J.D., Hatcher Jr., R.D., 1994. Controls on hinge-parallel extension fracturing in single-layer tangential-longitudinal strain fold. Journal of Geophysical Research 99, 22,027–22,041.
McNaught, M.A., Mitra, G., 1993. A kinematic model for the origin of footwall synclines. Journal of Structural Geology 15, 805–808.
Medwedeff, D.A., Suppe, J., 1997. Multibend fault-bend folding. Journal of Structural Geology 19, 279–292.
Mitra, S., 1987. Regional variations in deformation mechanisms and structural styles in the central Appalachian orogenic belt. Geological Society of America Bulletin 70, 1087–1112.
Mitra, S., 1990. Fault-propagation folds: geometry, kinematic evolution, and hydrocarbon traps. American Association of Petroleum Geologists Bulletin 74, 921–945.
Mosar, J., Suppe, J., 1992. Role of shear in fault-propagation folding. In: McClay, K.R. (Ed.), Thrust Tectonics. Chapman and Hall, London, pp. 123–132.
Murray Jr., G.H., 1968. Quantitative fracture study-Sanish Pool, McKenzie County, north Dakota. American Association of Petroleum Geologists Bulletin 52, 57–65.
Narr, W., Currie, J.B., 1982. Origin of fracture porosity—example from Altamont Field, Utah. American Association of Petroleum Geologists Bulletin 66, 1231–1247.
Price, N.J., 1966. Fault and Joint Development in Brittle and Semi-brittle Rocks. Pergamon Press, Oxford.
Ramsay, J.G., 1974. Development of chevron folds. Geological Society of America Bulletin 85, 1741–1754.
Salvini, F., Storti, F., 1997. Spatial and temporal distribution of fractured rock panels from geometric and kinematic models of thrust-related folding. American Association of Petroleum Geologists International Conference, Vienna, Abstracts, A51.
Sanderson, D.J., 1982. Models of strain variation in nappes and thrust sheets, a review. Tectonophysics 88, 201–233.
Srivastava, D.C., Engelder, T., 1990. Crack-propagation sequence and pore-fluid conditions during fault-bend folding in the Appalachian Valley and Ridge, central Pennsylvania. Geological Society of America Bulletin 102, 116–128.
Stearns, D.W., 1968. Certain aspects of fracture in naturally deformed rocks. In: Rieker, R.E. (Ed.), National Science Foundation advanced science seminar in rock mechanics. Special report, Air Force Cambridge Research Laboratories, Bedford, Massachusetts, AD66993751, pp. 97–118.
Stewart, K.G., Alwarez, W., 1991. Mobile-hinge kinking in layered rocks and models. Journal of Structural Geology 13, 243–259.
Storti, F., Salvini, F., 1996. Progressive rollover fault-propagation folding: a possible kinematic mechanism to generate regional-scale recumbent folds in shallow foreland belts. American Association of Petroleum Geologists Bulletin 80, 174–193.
Storti, F., Salvini, F., McClay, K., 1997. Fault-related folding in sandbox analogue models of thrust wedges. Journal of Structural Geology 19, 583–602.
Strayer, L.M., Hudleston, P.J., 1997. Numerical modeling of fold initiation at thrust ramps. Journal of Structural Geology 19, 551–566.
Suppe, J., 1983. Geometry and kinematics of fault-bend folding. American Journal of Science 283, 684–721.
Suppe, J., Medwedeff, D.A., 1984. Fault-propagation folding. Geological Society of America Bulletin, Abstracts with programs 16, 670.
Suppe, J., Medwedeff, D.A., 1990. Geometry and kinematics of fault-propagation folding. Eclogae Geologicae Helvetiae 83, 409–454.
Suppe, J., Chou, G.T., Hook, S.C., 1992. Rates of folding and faulting determined from growth strata. In: McClay, K.R. (Ed.), Thrust Tectonics. Chapman and Hall, London, pp. 105–121.
Thorbjornsen, K.L., Dunne, W.M., 1997. Origin of a thrust-related fold: geometric vs kinematic tests. Journal of Structural Geology 19, 303–319.
Weiss, L.E., 1980. Nucleation and growth of kink bands. Tectonophysics 65, 1–38.
Wickham, J., 1995. Fault-displacement-gradient folds and the structure at Lost Hills, California (U.S.A.). Journal of Structural Geology 17, 1293–1302.
Wilkerson, M.S., Medwedeff, D.A., Marshak, S., 1991. Geometrical modeling of fault-related folds: a pseudo-three-dimensional approach. Journal of Structural Geology 13, 801–812.
Wiltschko, D.V., Medwedeff, D.A., Millson, H.E., 1985. Distribution and mechanisms of strain within rocks on the northwest ramp of Pine

Mountain block, southern Appalachian foreland: a field test of theory. Geological Society of America Bulletin 96, 426–435.
Wojtal, S., 1986. Deformation within foreland thrust sheets by populations of minor faults. Journal of Structural Geology 8, 341–360.
Wojtal, S., Mitra, G., 1986. Strain hardening and strain softening in fault zones from foreland thrusts. Geological Society of America Bulletin 97, 674–687.
Woodward, N.B., Rutherford Jr., E., 1989. Structural lithic units in external orogenic zones. Tectonophysics 158, 247–267.